Sensorless Automatic Stop Control of Electric Vehicle in Semi-dynamic Wireless Charging System

Jirawat Sithinamsuwan, Kensuke Hanajiri, Katsuhiro Hata, Takehiro Imura, Hiroshi Fujimoto, Yoichi Hori
The University of Tokyo
5-1-5, Kashiwanoha, Kashiwa, Chiba, 277-8561 Japan
Email : sithinamsuwan.jirawat18@ae.k.u-tokyo.ac.jp

***Abstract*—Semi-dynamic wireless charging system provides electric power to electric vehicles (EVs) on the point of stopping. This paper proposes a scheme of positioning system in semi-dynamic wireless charging system via magnetic resonance coupling in order to perform sensorless automatic stop control in EVs by using parameters from wireless power transfer system (WPT). Furthermore, this proposed method also selects the stop position where occupies high transmission efficiency and short vehicular gap which leads to energy conservation and traffic jam problem reduction. The experiments demonstrated that the proposed method is able to stop the vehicle at the high transmission efficiency position without any visual sensor.**

***Index Terms*—Sensorless automatic stop, Wireless power transfer, Semi-dynamic wireless charging, Electric vehicle**

I. Introduction

Electric Vehicle (EV) is well known as the new choice for vehicles in the future as it reduces CO_2 emission. However, the common power source in EV, Li-ion battery is not able to provide energy as much as gasoline does. Thus, EVs normally occupy short range driving comparing to gasoline cars.

Some of advanced studies [1] apply WPT system to electric vehicle. Static wireless charging system was implemented as the first stage of WPT system in EVs. Still, static wireless charging system could not solve the EV's short driving range problem.

Semi-dynamic wireless charging system is one of the applications of WPT system. As shown in Fig. 1, performing power transmission while EV decelerates and stop its motion is called Semi-dynamic wireless charging [2]. For instance, if transmission equipment is installed beneath the road where is adjacent to the intersection with a traffic light, EVs are able to acquire electric power while they are waiting at the traffic light. This system is capable of providing sufficient electric power to extend the driving range of EVs [3].

Former researches [4], [5] proposed an sensorless automatic stop control at low speed (e.g. $\approx$ 10 mm/s) by PI control. Still, this control method is not applicable to practical velocity (e.g. $10\,\mathrm{km/h}$) and only able to stop the vehicle at the center of the coil. Effectiveness of the transmission (e.g. transmission efficiency) was not considered in these former researches.

This paper proposes the real-time sensorless automatic stop control in semi-dynamic wireless charging as well as stop position estimation algorithm. This proposed method is not only applicable to linear motion of EVs at practical velocity (e.g. $10\,\mathrm{km/h}$), but also applicable to the linear motion of EVs at inconstant velocity in order to perform the realistic automatic stop control. High transmission efficiency and short vehicular gap position is chosen to be the stop position aiming for energy conservation and traffic jam reduction.

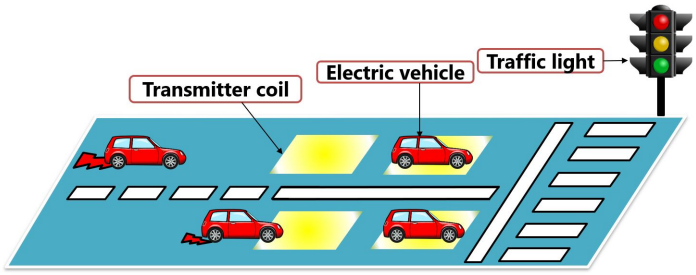

Fig. 1. Semi-dynamic wireless charging system in EVs

In this paper, sensorless automatic stop control algorithm is proposed. Then, the validity and the effectiveness of proposed method are presented by simulations and experiments on automatic stop control.

II. Sensorless Automatic Stop Control

A. Algorithm

This section explains the algorithm used in proposed method of automatic stop control in semi-dynamic wireless charging system without any visual sensor as shown in Fig. 2.

(a) Vehicle approaches a transmitter coil at velocity V_0.
(b) Vehicle is detected by WPT circuit parameters.
(c) Vehicle decelerates itself to intermediate velocity U_0.
(d) Vehicle estimates the stop position.
(e) Vehicle stops at high transmission efficiency position.

B. Stop Position Selection

In automatic stop control, vehicle will decelerate to stop at particular position. Each stop position provides different transmission power and transmission efficiency due to the change of mutual inductance between coils [6]. In this research, high transmission efficiency and short vehicular gap conditions are selected as the conditions of stop position.

In order to make proposed method simple to understand, consider a pair of coils with 10 cm gap length in Fig. 4 and WPT circuit parameters in Table III as simulation conditions.

Here, x is defined as the horizontal misalignment between the center of receiver coil and the center of transmitter

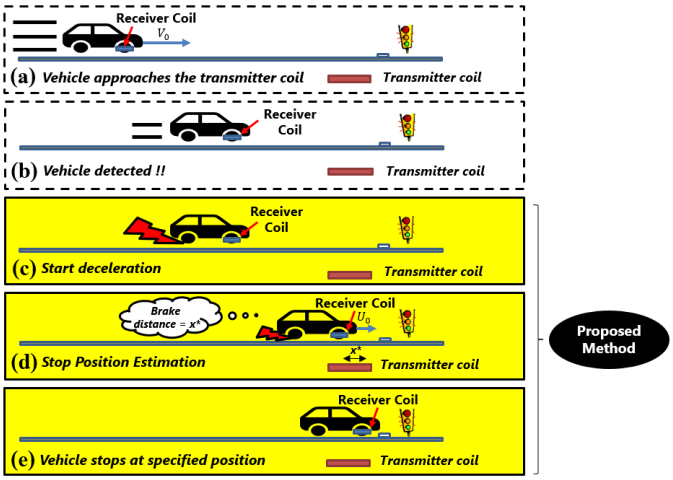

Fig. 2. Automatic stop control algorithm (this paper proposes (c) - (e))

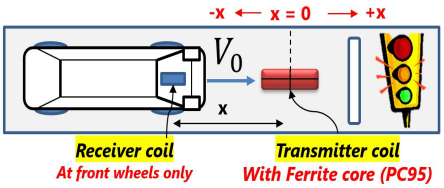

Fig. 3. Problem setting (top view)

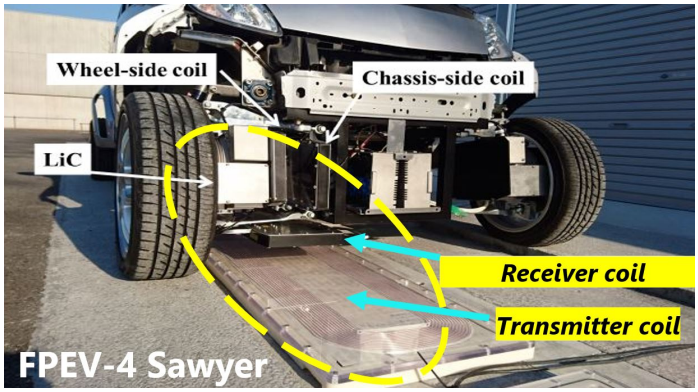

Fig. 4. Experiment transmitter coil and receiver coil

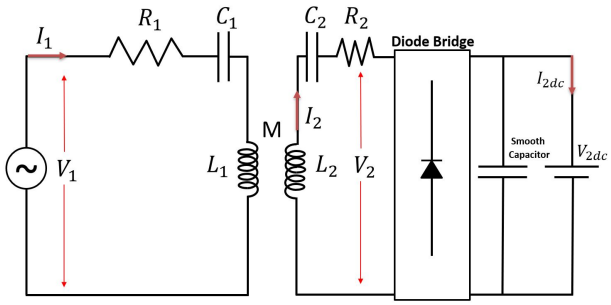

Fig. 5. Wireless Power Transfer (WPT) Equivalent Circuit

coil. On the half-left side of the transmitter coil, horizontal misalignment x is taken as $x < 0$. On the other hand, the half-right side of the transmitter coil, horizontal misalignment x is considered as $x > 0$ as shown in Fig.3.

Fig. 5 shows the equivalent circuit of WPT circuit used in this proposed method. Circuit parameters R_1, L_1, C_1, R_2, L_2 and C_2 are resistance, inductance, capacitance in primary and secondary side respectively.

Constant voltage source V_{2dc} is used as a load on secondary side in order to model battery charging in EVs. M is the mutual inductance between these two coils. In order to maximize the transmission efficiency, both coils ought to have the same resonance frequency ω_0 [7]. Resonance frequency condition is given in (1) [8].

$$\omega_0 = \frac{1}{\sqrt{L_1 C_1}} = \frac{1}{\sqrt{L_1 C_2}} \tag{1}$$

According to the circuit equation from WPT circuit in Fig. 5, root mean square value of alternating current (AC) on the primary side (transmitter coil) I_1 and secondary side (receiver coil) I_2 can be solved as shown in the following equation (2).

$$\begin{aligned} I_1 &= \frac{\omega_0 M V_2 + R_2 V_1}{R_1 R_2 + \omega_0^2 M^2} \\ I_2 &= \frac{\omega_0 M V_1 - R_1 V_2}{R_1 R_2 + \omega_0^2 M^2} \end{aligned} \tag{2}$$

From the current values in equation (2), transmitted power P_1, received power P_2 and transmission efficiency η are able to be expressed in the following equation (3) - (4) [9].

$$\begin{aligned} P_1 &= V_1 I_1 \\ P_2 &= V_2 I_2 \end{aligned} \tag{3}$$

$$\eta = \frac{P_2}{P_1} \times 100[\%] \tag{4}$$

Voltage source is given as $V_1 = V_2 = 110\,\mathrm{V}$ (nominal voltage in the USA). Mutual inductance M between a pair of coils at each position is able to be calculated by Neumann formula [10]. Finally, transmission efficiency η at each position of transmitter coil can be calculated from (2) - (4).

The simulation result (Fig. 6) indicates that if received current decreases, the transmission efficiency increases. Therefore, in this case, transmission efficiency reaches maximum value at horizontal misalignment $x = 400$ mm as shown in Fig. 6. Notice that the value of WPT parameters in Fig. 6 also depends on coil shape and gap length. Hence, transmission efficiency curve trend in Fig. 6 changes in case of different coil shape or gap length conditions.

TABLE I
WPT CIRCUIT PARAMETERS

Parameter	Transmitter coil	Receiver coil
Resistance [mΩ]	$R_1 = 342.5$	$R_2 = 383.3$
Inductance [μH]	$L_1 = 429$	$L_2 = 377.7$

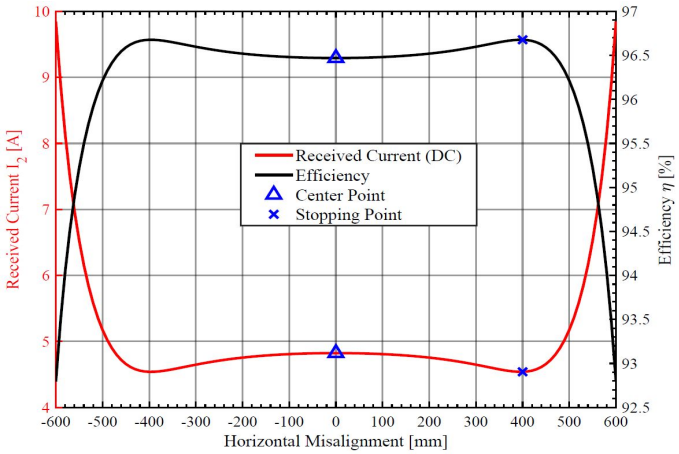

Fig. 6. Circuit parameters distribution simulation

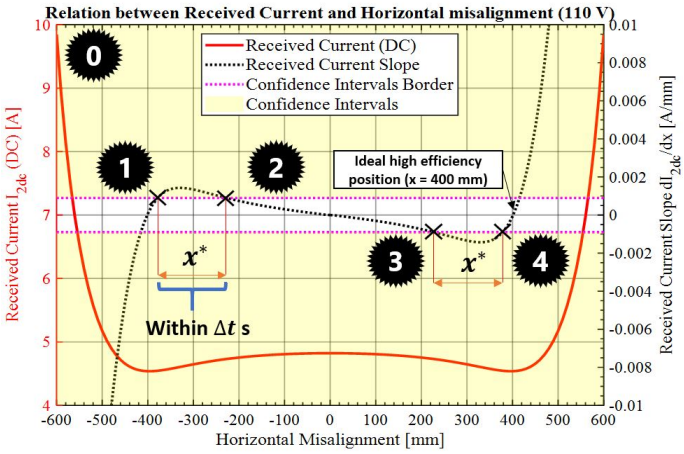

Fig. 7. Received current I_{2dc} gradient simulation

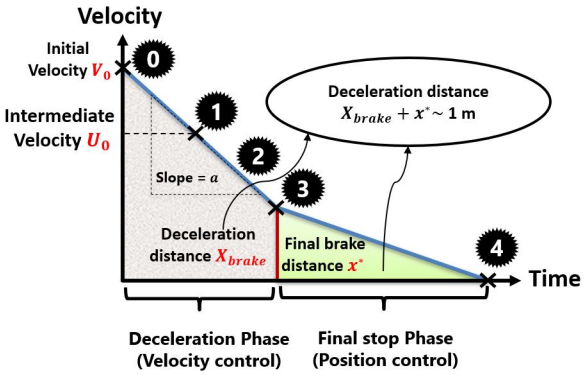

Fig. 8. Deceleration Model

C. Automatic Stop Control

*1) **Deceleration Phase (Position 0):***

As shown in Fig. 7, proposed automatic stop control starts when the vehicle has approached the position 0 where is safe to perform power transmission. Current at the transmitter coil I_1 increases when the received coil position is far away from the transmitter coil. Hence, unless the current at the transmitter coil I_1 is low enough, power transmission should not be performed in order to prevent the excess current [9]. This vehicle detection method is implemented by using search pulse of the inverter output voltage (V_1) on primary side [9].

After the vehicle has been detected , vehicle decreases its velocity with constant deceleration a by velocity control system as shown in Fig 8.

*2) **Stop Position Estimation (Position 1-2):***

As mentioned above, stop position has been determined at high transmission efficiency and short vehicular gap position. Stop position estimation algorithm is proposed since EVs need to define its stop position prior to automatic stop control.

Received current (DC) I_{2dc} is chosen as the vehicle detection parameter for automatic stop control since this parameter can be directly measured by current meter at secondary side of WPT circuit. In addition, received current (DC) has less fluctuation than alternating received current I_2.

Using received current (DC) gradient with horizontal misalignment dI_{2dc}/dx as a vehicle detection parameter is proposed in this research since gradient value becomes zero when received current value reaches local minimum or local maximum value. According to (2) - (4) and simulation result in Fig. 6, maximum transmission efficiency position and minimum received current position is the same position.

In other words, maximum transmission efficiency position is able to be specified by using received current gradient dI_{2dc}/dx.

However, received current gradient dI_{2dc}/dx is not completely reliable parameter. During the measurement, either environment noise or equipment error affects the measured current value and consequently causes variation in gradient value. As a result, low received current gradient is not significant due to the disturbance.

Therefore, confidence interval is introduced as criterion of received current gradient reliability as shown in simulation result (Fig. 7). Confidence interval border $\Delta I_{min}/\Delta x$ (pink dotted line in Fig. 7) can be determined by equation (5).

$$\pm\frac{\Delta I_{min}}{\Delta x} = \pm\frac{\Delta I_{min}}{\Delta T} \div \frac{\Delta x}{\Delta T} = \pm\frac{\Delta I_{min}}{\Delta T} \div V \qquad (5)$$

Here, ΔI_{min} , ΔT and V are given as the current meter maximum resolution, gradient calculation sampling time and vehicle velocity respectively. In order to judge the reliability of measured received current gradient dI_{2dc}/dx, the following conditions (6) - (7) are proposed.

$$\left|\frac{dI_{2dc}}{dx}\right| > \frac{\Delta I_{min}}{\Delta x} \qquad (6)$$

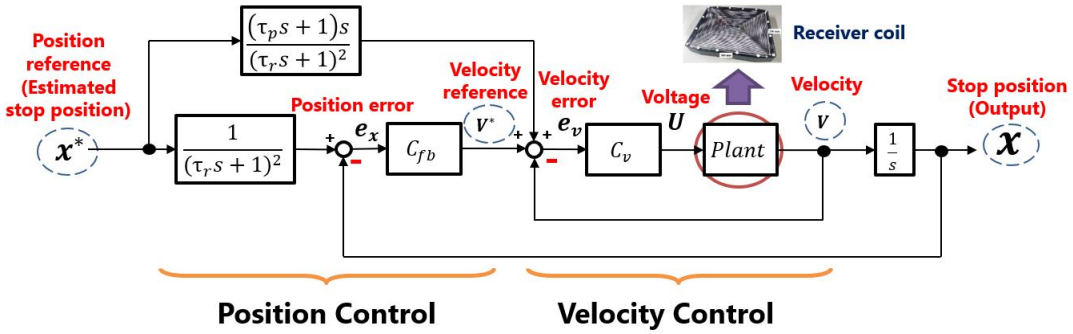

Fig. 9. Two-degree of freedom control system block diagram

TABLE II
CONTROL PARAMETERS IN BLOCK DIAGRAM

Symbol	Variable
C_{fb}	Feedback controller
C_v	Velocity controller
τ_r	Constant time for low-pass filter
τ_p	Constant time for velocity controller
s	Laplace operator

$$\left|\frac{dI_{2dc}}{dx}\right| < \frac{\Delta I_{min}}{\Delta x} \tag{7}$$

Measured received current gradient dI_{2dc}/dx (black dotted line in Fig. 7) becomes reliable when (6) is satisfied because it is greater than the confidence interval border. On the other hand, dI_{2dc}/dx becomes unreliable when (7) is satisfied since the measured value dI_{2dc}/dx is less than the confidence interval border and that might be considered as the effect from the disturbance.

In Fig. 7, vehicle will be detected at position 1 when received current gradient dI_{2dc}/dx exceeds the confidence interval border for the first time. Meanwhile, the timer starts right after vehicle has passed position 1. This timer will be finished as soon as received current gradient dI_{2dc}/dx falls below the confidence interval at position 2. Since we know the vehicle's intermediate velocity U_0 at position 1 from Fig. 8 and time during position 1 and 2 (Δt) from Fig. 7, distance x^* between position 1 and 2 can be simply calculated from the following equation (8).

$$x^* = U_0 \Delta t - \frac{1}{2} a (\Delta t)^2 \tag{8}$$

According to the coil characteristics symmetry, after vehicle has passed the position 2, the parameter on right-half side ($x > 0$) is considered to be the same as the one on left-half side of the transmitter coil. On the right-half side, automatic control system starts when vehicle enters confidence interval at position 3 (when $dI_{2dc}/dx < -I_{min}/\Delta x$).

*3) **Final stop phase (Position 3-4)**:*

As shown in Fig. 7 - 8, final stop position control starts from position 3. Estimated brake distance x^* is used as an input of control system. Two-degree of freedom control method was adapted in automatic stop control system as shown in Fig. 9. This block diagram consists of position and velocity control. Each parameter in Fig. 9 is described above in Table II. Feedforward controller gives control system the capability to follow the command input x^* (control system input) and feedback controller reduces overshoot in set-point response x and suppresses the disturbance [11].

By using x^* as a command input of control system. Vehicle will be eventually controlled to stop at position 4 where is close by the local minimum received current position as shown in Fig. 6 (local maximum transmission efficiency position). Besides, this algorithm leads the vehicle to stop at position 4 rather than position 1 even it occupies the same transmission efficiency value as position 4 is more desirous since this position gives shorter vehicular gap.

Therefore, the confidence interval border plays an important role in the stop position estimation and automatic stop control. If confidence interval does not contain the local minimum and maximum of dI_{2dc}/dx, this stop position estimation method is unable to be used.

Moreover, confidence interval border changes in case of inconstant velocity motion due to (5). Gradient calculation sampling time ΔT needs to be adjusted in order to prevent confidence interval border variation during deceleration. If confidence interval border value is not appropriately determined, this system is not able to implement the accurate automatic stop control.

III. EXPERIMENT ON AUTOMATIC STOP CONTROL

A. Experiment setup

Aforementioned in Section I, the proposed method aims for high efficiency and short vehicular gap positioning in EV without any sensor equipment. Semi-dynamic wireless charging system's experiment setups in this research are explained below.

In this paper, experiment on bench model was implemented which represents the one-dimensional motion of electric vehicle (Fig. 10(a)). From now on, let's define that receiver coil on bench represents the EV.

The transmitter coil, receiver coil and WPT equivalent circuit are shown in Fig. 4 - 5 respectively. Resistance and inductance of primary and secondary side circuit are shown

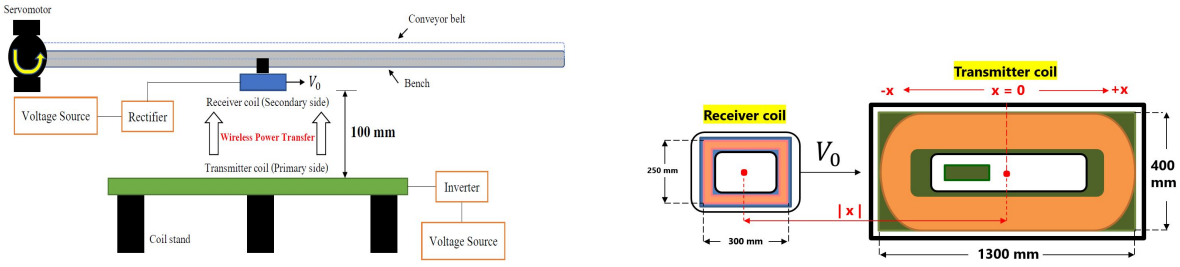

(a) Experiment setup (side view)

(b) Experiment setup (top view)

Fig. 10. Experiment equipment setup

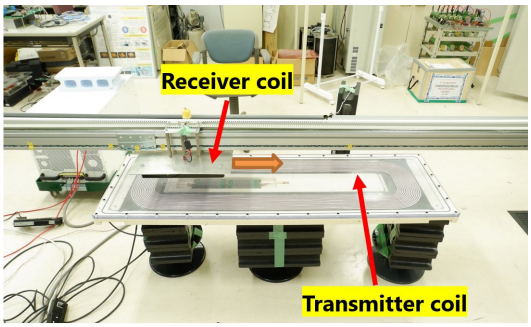

Fig. 11. Receiver coil in motion

in Table III. Resonance frequency of both coils is given as $f_0 = 85\,\mathrm{kHz}$. Voltage sources in primary side V_1 and secondary side V_2 are matched equally since the transmission efficiency increases by setting $V_1 = V_2$ [12].

The experiment's condition is shown Fig. 3. The vehicle approaches from the left side of transmitter coil ($x < 0$) at speed $V_0(4.7\,\mathrm{km/h}, 7.1\,\mathrm{km/h}$ and $9.4\,\mathrm{km/h})$ and move toward the traffic light located on the right side of the transmitter coil ($x > 0$). Vertical misalignment is not concerned in this experiment. The WPT system is subject to the below conditions.

- WPT is conducted by magnetic resonance coupling.
- Self-inductance of two coils remain constant.
- Coils characteristics are symmetry.
- Smooth capacitance is set to 4700 μF.
- Transmission occurs between a pair of coils with transmission gap $100\,\mathrm{mm}$ in steady state.

The experiment is validated by bench test drive equipment which receiver coil represents the EV as shown in Fig. 11. The receiver coil was driving to stop at specific position ($x \approx 400$ mm). Meanwhile, wireless power transmission was performed to measure received current (DC) I_{2dc}. Measured received current and its gradient are compared with simulation result in Fig. 6, 7. This experiment was conducted ten times for each velocity in order to investigate the certainty of this proposed method.

TABLE III
STOP POSITION ERROR ANALYSIS

Parameter \ Velocity	4.7 km/h	7.1 km/h	9.4 km/h
Mean (mm)	412.79	430.37	483.52
S.D. (mm)	5.38	8.91	2.25
RMSE (mm)	13.87	31.65	86.43

B. Experiment result

The received current waveform from bench test drive experiment results is shown in Fig. 12. Fig. 13 shows that the receiver coil gradient with receiver coil displacement has the similar trend to simulation result in Fig. 7. This means the simulation result is validated by the experiment and deceleration distance x^* was estimated. As long as confidence interval is defined properly and contains local maximum and minimum value of received current gradient, automatic stop control mentioned in the previous section is considered to be feasible.

Fig. 12-13 are one of the experiment results for each velocity. From Fig. 12 and Fig. 13, final estimated stop position is considered to be desired position comparing to the center of the coil because the received current at the stop position is lower than the value at the center of the coil, which means transmission efficiency at stop position is greater than the transmission efficiency at the center of the coil.

The stop position error analysis result is shown in Table III. The greater velocity the receiver coil moves, the more stop position error it becomes. On the average, the receiver coil stops before reaching the ideal stop position shown in simulation result (Fig. 6). However, the receiver coil was able to pass through the center of the coil and stop at the position closed by x = 400 mm (maximum transmission efficiency position).

As mentioned before, semi-dynamic wireless charging system provides electric power from deceleration until stop of EV (e.g. during braking and waiting traffic light). Therefore, if we assume that EVs stop at the power transmission area for a moment, this proposed method is able to reduce the total consumption energy during the wireless power transmission comparing to the other stop positions.

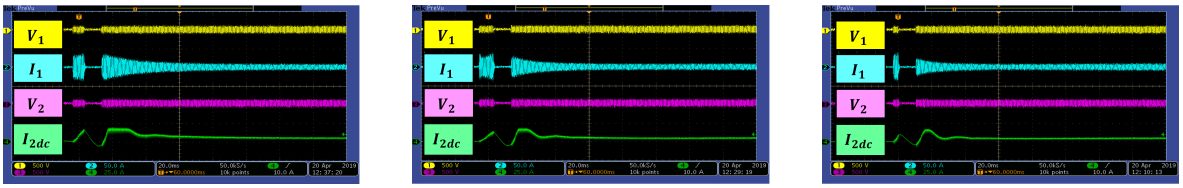

(a) V_0 = 4.7 km/h (b) V_0 = 7.1 km/h (c) V_0 = 9.4 km/h

Fig. 12. Oscilloscope Waveform (Experiment Result)

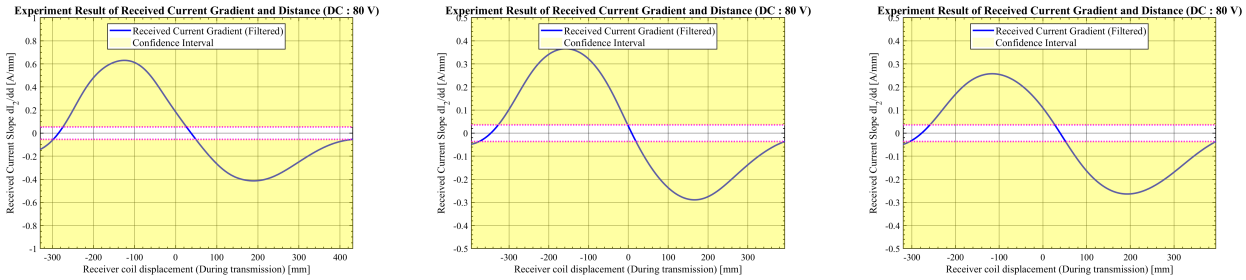

(a) V_0 = 4.7 km/h (b) V_0 = 7.1 km/h (c) V_0 = 9.4 km/h

Fig. 13. Received Current Gradient (Experiment Result)

IV. CONCLUSION AND FUTURE WORK

This paper presented an sensorless automatic stop control in semi-dynamic wireless charging in EV using the received current gradient. High transmission efficiency and short vehicular gap position is able to be detected when received current gradient decreases to zero. Stop position estimation algorithm is also applicable to inconstant velocity motion. The feasibility of the proposed method is validated by the bench test experiment. The experiment result shown that the proposed method is able to perform the position control to move the receiver coil to the high transmission efficiency position.

Future work consists of automatic stop control by more effective algorithm since the received current gradient parameter is not able to provide enough performance certainty for the application in real life. Moreover, complicated stop scene can also be considered. For examples, two-dimensional motion control ought to be considered in order to implement the practical automatic stop in electric vehicle as well. Therefore, lateral misalignment, gap length and the coil shape effect on automatic stop control performance needs to be examined in the next step of this research.

ACKNOWLEDGMENT

The author would like to appreciate the contributions of Toyo Denki Seizo K.K. and NSK Ltd. This paper was partly supported by JSPS KAKENHI Grant Number 17H04915, 18H03768, 19H02123 along with JST-Mirai Program Grant Number JP-MJMI17EM, Japan.

REFERENCES

[1] G. Daisuke, “Basic Study of Transmitting Power Control Method Without Signal Communication for Wireless In-Wheel Motor via Magnetic Resonance Coupling”, *IEEE International Conference on Mechatronics (ICM)* ,pp.1-6, 2015

[2] A. Zaheer and Grant A. Covie, “A Comparative Study of Various Magnetic Design Topologies for A Semi-Dynamic EV Charging Application” ,*IEEE 2nd Annual Southern Power Electronics Conference (SPEC)* , pp.1-6, 2016

[3] Omer C. Onar, John M. Miller, Steven L. Campbell, Chester Coomer, Cliff. P. White, and Larry E. Seiber, “A Novel Wireless Power Transfer for In-Motion EV/PHEV Charging” ,*IEEE Applied Power Electronics Conference and Exposition (APEC)* , pp.3073-3079, 2013

[4] P. Kotchapansompote, W. Yafei, T. Imura, H. Fujimoto, Y. Hori, “Electric Vehicle Automatic Stop using Wireless Power Transfer Antennas”, *IECON 2011 - 37th Annual Conference of the IEEE Industrial Electronics Society*, pp. 1-6, 2011

[5] P. Sukprasert, B. Minh Nguyen, H. Fujimoto, “Estimation and Control of Lateral Displacement of Electric Vehicle Using WPT Information” ,*IEEE International Conference on Mechatronics (ICM)* ,pp.1-6, 2015

[6] M. Sato, G. Yamamoto, T. Imura, H. Fujimoto, “Development of Wireless In-Wheel Motor Using Magnetic Resonance Coupling”, *IEEE Transactions on power electronics, Vol. 31, NO. 7, JULY 2016* ,pp.1-6, 2016

[7] K. Kusaka, J. Itoh, “Development Trends of Inductive Power Transfer Systems Utilizing Electromagnetic Induction with Focus on Transmission Frequency and Trasmission Power”, IEEJ Journal of Industry Applications, Vol.6, No.5, pp.334 2017

[8] G. Lovison , D. Kobayashi, M. Sato, T. Imura, Y. Hori, “Secondary-side only Control for High Efficiency and Desired Power with Two Converters in Wireless Power Transfer Systems”, IEEJ Journal of Industry Applications, Vol.6, No.6, pp.474 2017

[9] K. Hata , K. Hanajiri, T. Imura, H. Fujimoto, Y. Hori, M.Sato, D. Gunji,“Design and Implementation of Sensorless Vehicle Detection System for In-motion Wireless Power Transfer”, EVS 31 & EVTeC 2018, Kobe, Japan, pp.1-6 2018

[10] C. L. W. Sonntag, E. A. Lomonova, and J. L. Duarte , “Implementation of the Neumann Formula for Calculating the Mutual Inductance between Planar PCB Inductors” , *IEEE International Conference on Electrical Machines 2008*,pp.1-6

[11] M. Araki, H. Taguchi, “Two-Degree-of-Freedom PID Controllers”, *International Journal of Control, Automation, and Systems Vol. 1, No. 4, December 2003*, pp.401-410

[12] K. Hata , T. Imura , Y. Hori, “Proposal of Classification and Design Strategies for Wireless Power Transfer Based on Specification of Transmitter-Side and Receiver-Side Voltages and Power Requirements”, *IEEJ Transactions on Industry Applications 2018*, Vol. 138, No.4, pp.330-339,